

Theory of a mode-locked atom laser with toroidal geometry

Peter D. Drummond,¹ Antonios Eleftheriou,² Kerson Huang,² and Karen V. Kheruntsyan¹

¹*Department of Physics, University of Queensland, Brisbane, Qld 4072, Australia*

²*Department of Physics and Center for Theoretical Physics, Massachusetts Institute of Technology, Cambridge, Massachusetts 02139*

(Received 16 August 2000; revised manuscript received 9 January 2001; published 13 April 2001)

We consider a possible technique for mode locking an atom laser, based on the generation of a dark soliton in a ring-shaped Bose-Einstein condensate, with repulsive atomic interactions. The soliton is a kink, with angular momentum per particle equal to $\hbar/2$. It emerges naturally when the condensate is stirred at the soliton velocity and cleansed with a periodic out coupler. The result is a replicating coherent field inside the atom laser, stabilized by topology. We give a numerical demonstration of the generation and stabilization of the soliton.

DOI: 10.1103/PhysRevA.63.053602

PACS number(s): 03.75.Fi, 05.30.Jp, 05.45.Yv, 32.80.Pj

I. INTRODUCTION

The discovery of Bose-Einstein condensation (BEC) in ultracold alkali-metal vapors [1] in a magnetic trap, at temperatures of 10^{-6} K or lower, has raised the possibility of a coherent atom laser. Recent experimental [2] and theoretical [3] developments show that this is indeed practical. Most atom lasers to date, however, produce output pulses that are not obviously phase coherent. It would be desirable to have a mode-locked laser, in which the pulses are in phase with each other, for this will enable a wide range of interference experiments and phase-sensitive measurements. In addition, mode-locked lasers can have an enhanced intensity stability, relative to their nonmode-locked cousins. A possible technique for mode locking was demonstrated by Anderson and Kasevich [4], using accelerated motion in an atom-wave Bragg grating formed with an optical standing wave. However, this method was limited to very low densities in order to avoid atom-atom interactions.

Another way to make a mode-locked atom laser is to create a periodic field circulating around a ring-shaped condensate, and out couple it with a synchronized period. To do this, we must choose a periodic field that can be easily created and that has sufficient stability to enable a steady-state out-coupling process. In this regard, we suggest a dark soliton in a condensate of atoms with repulsive interactions. This is a kink configuration, which stands apart from a continuum of possible excitations, owing to two distinctive features: (a) It has a characteristic propagating velocity v ; (b) the angular momentum per particle, normal to the plane of the ring, is $\hbar/2$. Soliton techniques, which are often used in optical mode-locked lasers, have the intrinsic advantage that they are not limited to low densities, since the soliton formation itself is a nonlinear process.

The dark soliton can be created by stirring the condensate at the characteristic velocity v ; but it has to be cleaned up because the stirring also creates other excitations such as phonons. The cleansing can be achieved by applying a stroboscopic loss mechanism, which also serves as out coupler for the atom laser. The soliton persists because of topological stability associated with the half-integer angular momentum. In the following, we first describe the soliton as a solution of the nonlinear Schrödinger equation (NLSE), and then dem-

onstrate mode locking via numerical simulations.

II. NONLINEAR SCHRÖDINGER EQUATION ON A RING

Consider a condensate contained in a ring of radius R . Let the cross-sectional radius be r_0 , and let the cross-sectional area be denoted by $A = \pi r_0^2$. We choose $R \gg r_0$, so that the transverse excitations are far more energetic than those along the ring. For the low excitation modes, therefore, we may regard the condensate as a one-dimensional system, and denote by θ the angle around the ring. The condensate wave function $\Psi(\theta, t)$ satisfies the NLSE

$$i\hbar \frac{\partial \Psi}{\partial t} = -\frac{\hbar^2}{2mR^2} \frac{\partial^2 \Psi}{\partial \theta^2} + V(\theta)\Psi + \frac{4\pi\hbar^2 a}{m} |\Psi|^2 \Psi, \quad (2.1)$$

where m is the atomic mass, a the s -wave scattering length, and V is an external potential due to trap nonuniformity. The total number of atoms N enters through the normalization

$$AR \int_{-\pi}^{\pi} d\theta |\Psi|^2 = N, \quad (2.2)$$

which is a constant of the motion if V is independent of time. Continuity requires the boundary condition

$$\Psi(\theta + \pi, t) = \Psi(\theta - \pi, t). \quad (2.3)$$

The NLSE on a line is well known in nonlinear optics, where it describes the envelope of an electromagnetic wave propagating along an optical fiber [5]. Let us recount what is generally known in the one-dimensional case. For attractive interactions with $\alpha < 0$, the nonlinear term in the equation presents an attractive potential proportional to $|\Psi|^2$. In three spatial dimensions in free space this would lead to “self-focusing”—the development of spots of infinite intensity in finite time [6]. In one dimension, however, the kinetic energy counterbalances the attraction leading to the formation of a stable bright soliton. The situation is the same when we join the ends of the line to form a ring.

For repulsive interactions with $\alpha > 0$, we can make a dark soliton in a linear condensate by requiring Ψ to approach

± 1 at opposite ends of the line. By continuity, the configuration must have a kink, i.e., a zero of the wave function. The slope at the kink determines its propagation velocity v , which will be finite and nonzero. Gray solitons also exist, in which the wave function has a minimum, but never vanishes. These have been analyzed theoretically [7], and created experimentally [8,9]. They propagate with a speed proportional to the wave intensity at the minimum, and hence come to rest in the dark-soliton limit.

These belong to a different class from the kink soliton we are considering on a ring, where periodicity demands that the ends match. Therefore, the phase of the wave function must change by $n\pi$ upon one complete revolution, where n is an odd integer. This makes the angular momentum per particle normal to the ring $n\hbar/2$, for the same mathematical reason that an electron has spin 1/2. The lowest-energy dark soliton has $n=1$.

It is convenient to use dimensionless variables to reduce the NLSE to the form

$$i\frac{\partial\psi}{\partial\tau} = -\frac{\partial^2\psi}{\partial\theta^2} + \mathcal{V}\psi + \alpha|\psi|^2\psi, \quad (2.4)$$

where

$$\begin{aligned} \psi &\equiv \Psi \sqrt{2\pi AR/N}, \\ \tau &\equiv (\hbar/2mR^2)t, \\ \mathcal{V} &\equiv (2mR^2/\hbar^2)V, \\ \alpha &\equiv 4NRa/A. \end{aligned} \quad (2.5)$$

In our work, we consider a ring-shaped condensate with $\mathcal{V}=0$.

The boundary condition is

$$\psi(\theta + \pi, \tau) = \psi(\theta - \pi, \tau), \quad (2.6)$$

and the normalization condition is

$$\int_{-\pi}^{\pi} d\theta \psi^* \psi = 2\pi. \quad (2.7)$$

The dimensionless energy per particle ϵ and angular momentum per particle j normal to the ring are given by

$$\begin{aligned} \epsilon &= \frac{1}{2\pi} \int_{-\pi}^{\pi} d\theta \left[\frac{\partial\psi^*}{\partial\theta} \frac{\partial\psi}{\partial\theta} + \mathcal{V}\psi^*\psi + \frac{\alpha}{2}(\psi^*\psi)^2 \right], \\ j &= \frac{1}{4\pi i} \int_{-\pi}^{\pi} d\theta \left(\psi^* \frac{\partial\psi}{\partial\theta} - \psi \frac{\partial\psi^*}{\partial\theta} \right). \end{aligned} \quad (2.8)$$

We shall first discuss the uniform vortex solutions, and then derive the soliton solutions. We analyze the mathematical properties of the solitons, and then discuss their use in an atom laser, which necessitates adding gain and loss terms in the equation of motion. The feasibility of a mode-locked atom laser will be demonstrated through numerical simulations.

III. UNIFORM SOLUTIONS

We first examine uniform solutions. For a uniform state, in the case of repulsive interaction ($\alpha > 0$) and zero external potential, we must clearly have (by the normalization condition)

$$\psi^* \psi = 1. \quad (3.1)$$

The lowest-energy solution is just the uniform condensate, which evolves in time according to

$$\psi_0(\theta, \tau) = e^{-i\omega_0\tau}, \quad (3.2)$$

where the dimensionless frequency is given by $\omega_0 = \alpha$. The corresponding dimensionless energy is $\epsilon_0 = \alpha/2$.

Next, consider solutions whose phase changes linearly around the circumference of the torus. We can call these the uniform vortex states. They correspond to the entire condensate having an angular momentum l , giving rise to the condensate wave function

$$\psi_l(\theta, \tau) = e^{-i\omega_l\tau + il\theta}, \quad (3.3)$$

where l must be an integer, in order to satisfy the boundary condition. The equation of motion gives

$$\omega_l = \alpha + l^2. \quad (3.4)$$

The dimensionless energy and dimensionless momentum per particle of the uniform vortex state are

$$\begin{aligned} \epsilon &= \alpha/2 + l^2, \\ j &= l \quad (l = 1, 2, 3, \dots). \end{aligned} \quad (3.5)$$

These are the simplest vortices, since they describe a circulation around the circumference of the ring. They have no phase singularity, since the center of the ring is not accessible to the BEC. The circulation is quantized; for these solutions to occur, each particle must have an integer angular momentum, so the whole system has an angular momentum of $Nl\hbar$ in physical units. Another way to think about this is that each particle is in the same quantum state, with integer angular momentum quantum number.

A. Phonons

We can obtain the phonon spectrum of small fluctuations around either the ground state or the uniform vortex, as follows. Perturb the vortex state by writing

$$\psi(\theta, \tau) = \psi_l(\theta, \tau) [1 + \delta\psi(\theta, \tau)] \quad (3.6)$$

and obtain the linearized equation

$$\begin{aligned} i\frac{\partial}{\partial\tau} \delta\psi &= -\frac{\partial^2}{\partial\theta^2} \delta\psi + \alpha[\delta\psi + \delta\psi^*] \\ &\quad - 2il\frac{\partial}{\partial\theta} \delta\psi + (l^2 - l)\delta\psi. \end{aligned} \quad (3.7)$$

This can be solved by putting

$$\begin{aligned}\delta\psi &= Ue^{-i\lambda} + V^*e^{i\lambda}, \\ \lambda &= \delta\omega\tau - n\theta.\end{aligned}\quad (3.8)$$

We then obtain the phonon dispersion law, which is similar to that of Bogoliubov [10]

$$\delta\omega = n(2l + \sqrt{n^2 + 2\alpha}), \quad (3.9)$$

where n is an integer, in order to satisfy the periodic boundary condition. Note that unlike an infinite uniform BEC the phonon spectrum is discrete. In other words, there is no continuum of phonons at low frequency. This is a generic property of finite trap geometries.

IV. SOLITONS IN A RING

The one-dimensional NLSE is known to be classically integrable and to have periodic soliton solutions that correspond to localized disturbances traveling around the circumference of the torus. For configurations that move around the ring, we denote the angle in the comoving frame by

$$\bar{\theta} = \theta - v\tau, \quad (4.1)$$

and seek solutions of the form

$$\psi(\theta, \tau) = f(\bar{\theta})e^{i\eta(\bar{\theta}, \tau)}. \quad (4.2)$$

Here v is an arbitrary real parameter corresponding to the soliton velocity in our dimensionless variables. In general, a continuous set of velocities is possible. Complex values of f correspond to gray solitons having noninteger velocities. Real values of f correspond to dark and bright solitons having integer values of v . The definition of f as having no time dependence in the moving frame is a strong restriction that will allow soliton solutions that are shape-invariant, but excludes time-varying multiple-soliton solutions.

The resulting equations of motion are

$$v \frac{\partial f}{\partial \bar{\theta}} = 2 \frac{\partial f}{\partial \bar{\theta}} \frac{\partial \eta}{\partial \bar{\theta}} + f \frac{\partial^2 \eta}{\partial \bar{\theta}^2}, \quad (4.3)$$

$$\left[\frac{\partial \eta}{\partial \tau} - v \frac{\partial \eta}{\partial \bar{\theta}} \right] f = \left[\frac{\partial^2 f}{\partial \bar{\theta}^2} - f \left(\frac{\partial \eta}{\partial \bar{\theta}} \right)^2 \right] - \alpha f |f|^2.$$

Assume the form

$$\eta(\bar{\theta}, \tau) = l\bar{\theta} - \omega\tau, \quad (4.4)$$

where ω is the angular frequency of the condensate phase as observed in the rotating frame. The first equation of motion requires

$$v = 2l. \quad (4.5)$$

The equation for $f(\bar{\theta})$ then reads

$$f'' = \frac{\partial^2 f}{\partial \bar{\theta}^2} = \alpha f |f|^2 - \beta f, \quad (4.6)$$

where we have introduced a new parameter β equivalent to a dimensionless chemical potential defined as

$$\beta \equiv \omega + l^2. \quad (4.7)$$

The dimensionless classical field energy is given by

$$\begin{aligned}\epsilon &= \frac{1}{2\pi} \int_{-\pi}^{\pi} d\theta \left[|f'|^2 + l^2 |f|^2 + \frac{\alpha}{2} |f|^4 \right] \\ &= \beta + l^2 - \frac{\alpha}{4\pi} \int_{-\pi}^{\pi} d\theta |f|^4.\end{aligned}\quad (4.8)$$

Here the second expression was obtained by using the properties of the equation of motion and the normalization condition, together with the usual result that

$$f^* f'' = \alpha |f|^4 - \beta |f|^2 = \frac{\partial}{\partial \theta} (f^* f') - \left| \frac{\partial f}{\partial \theta} \right|^2. \quad (4.9)$$

We can also add these two expressions for the energy to obtain a third expression in which the quartic term does not appear,

$$\epsilon = \frac{\beta}{2} + l^2 + \frac{1}{4\pi} \int_{-\pi}^{\pi} d\theta \left| \frac{\partial f}{\partial \theta} \right|^2. \quad (4.10)$$

From its equation of motion, the quantity $f = f_x + if_y$ is the complex coordinate of a Newtonian particle of unit mass moving in a two-dimensional potential $V(f)$ given by

$$V(f) = -\frac{\alpha}{4} (f_x^2 + f_y^2)^2 + \frac{\beta}{2} (f_x^2 + f_y^2) = -\frac{\alpha}{4} |f|^4 + \frac{\beta}{2} |f|^2. \quad (4.11)$$

The conserved ‘‘energy’’ for this equivalent Newtonian motion is

$$E = |f'|^2/2 + V(f). \quad (4.12)$$

A. Real solutions

In the case of a real envelope function, which we mostly treat here, the boundary condition demands

$$f(\bar{\theta} + \pi) = (-1)^{2l} f(\bar{\theta} - \pi), \quad (4.13)$$

$$\eta(\theta + \pi, \tau) = \eta(\theta - \pi, \tau) + 2\pi l,$$

where $l = 0, \pm \frac{1}{2}, \pm 1, \pm \frac{3}{2}, \pm 2, \dots$ in order to satisfy the boundary condition. The angular momentum is

$$j = l = 0, \pm \frac{1}{2}, \pm 1, \pm \frac{3}{2}, \pm 2, \dots, \quad (4.14)$$

The solution can be obtained exactly via the energy integral

$$\int \frac{df}{\sqrt{2[E-V(f)]}} = \int d\bar{\theta}. \quad (4.15)$$

For repulsive interaction $\alpha > 0$, there exist bounded motions between turning points $\pm f_1$. This means that f has a zero and corresponds to a kink or dark soliton. For attractive interaction $\alpha < 0$, the bounded motion occurs between f_2 and f_1 with $f_2 > f_1 > 0$ and gives a bright soliton.

It is also possible to have a stationary solution, which corresponds to the previous uniform solutions. These must have $f=1$ due to our normalization condition, which means that $\beta = \alpha$, and hence that $\omega = \alpha - l^2$ in the co-moving frame. Transforming back to the laboratory frame gives the result that $\omega_l = \alpha + l^2$, as obtained previously.

B. Complex solutions

A gray soliton is possible only if f is complex. This case can be treated either by solving the full two-dimensional Newtonian motion problem or else by reducing the problem further on taking into account the rotational symmetry in the resulting two-dimensional effective potential. This leads to an effective ‘‘internal’’ angular momentum L that is also conserved (like E). To take this into account, we may redefine the phase η so that it includes the phase term previously included in f due to the internal motion. Assume the form

$$\eta(\bar{\theta}, \tau) = l_0 \bar{\theta} - \omega \tau + L \int f^{-2}(\bar{\theta}) d\bar{\theta}, \quad (4.16)$$

then the equation for f can be reduced to a real equation

$$f'' = \alpha f^3 - \beta f + L^2/f^3, \quad (4.17)$$

where now $v = 2l_0$ and $\beta = \omega + l_0^2$. However, the term l_0 is no longer necessarily the orbital angular momentum of the background condensate, since there is additional angular momentum carried in the extra phase term. This extra term generates a centrifugal barrier term in the equation of motion proportional to L^2 that corresponds to the effective potential

$$V_{eff}(f) = -\frac{\alpha}{4}f^4 + \frac{\beta}{2}f^2 + \frac{L^2}{2f^2}. \quad (4.18)$$

In the case $L \neq 0$, the centrifugal barrier means that f cannot change sign, so that

$$\begin{aligned} f(\bar{\theta} + \pi) &= f(\bar{\theta} - \pi), \\ \eta(\theta + \pi, \tau) &= \eta(\theta - \pi, \tau) + 2\pi l, \end{aligned} \quad (4.19)$$

where $l = 0, \pm 1, \pm 2, \dots$ in order to satisfy the boundary condition. It is no longer necessary for l_0 to have integer or half-integer values, since part of the total phase shift now comes from the ‘‘internal’’ phase shift. As before, the solution can be obtained via the energy integral. For repulsive interaction $\alpha > 0$, there exist bounded motions between turning points f_1, f_2 . This means that f has no zero and corresponds to a gray soliton.

C. Gray solitons and phonons

The gray solitons reduce to the previously obtained phonon solutions in the limit of small amplitude motion for the repulsive case of $\alpha > 0$. In order to see this, consider the low-amplitude solutions of the Newton equations near a minimum in the effective potential. At this minimum point where $f = f_0$,

$$L^2 = f_0^4(\beta - \alpha f_0^2). \quad (4.20)$$

Expanding around the minimum at $f = f_0$ gives an approximate equation for small amplitude motion

$$f'' = -(f - f_0)V''(f_0), \quad (4.21)$$

where the second derivative of the potential is

$$V''(f_0) = -6\alpha f_0^2 + 4\beta > 0. \quad (4.22)$$

A resulting solution for f that satisfies the boundary conditions in the limit of small oscillations with amplitude A has $f_0 = 1$, and

$$f = 1 + A \cos(n\bar{\theta}) + O(A^2). \quad (4.23)$$

The periodicity requirement on f means that n is an integer with

$$n^2 = V''(f_0) = 4\beta - 6\alpha f_0^2, \quad (4.24)$$

and the phase solution is

$$\eta(\bar{\theta}, \tau) = l_0 \bar{\theta} - \omega \tau + L \int \frac{1}{[1 + A \cos(n\bar{\theta})]^2} d\bar{\theta} \quad (4.25)$$

$$\simeq (l_0 + L)\bar{\theta} - \omega \tau - \frac{2LA}{n} \sin(n\bar{\theta}). \quad (4.26)$$

The periodicity requirement on the phase-term η means that $l = l_0 + L$ is an integer, as expected. In this limit we also recover the relationship that the total angular momentum is $j = l$, although this is not generally true for gray solitons. We can also calculate from the conditions on the minimum that $L = \pm \sqrt{\beta - \alpha}$, where the properties of the potential minimum mean that $\beta = (n^2 + 6\alpha)/4$. In order to compare this with the usual linearized solution, we choose the negative root for L , and note that the additional oscillation frequency due to the gray soliton is identical to the linearized solution of the original equations,

$$\delta\omega = 2nl_0 = 2n(l + \sqrt{\beta - \alpha}) = n(2l + \sqrt{n^2 + 2\alpha}). \quad (4.27)$$

This result demonstrates that a low-amplitude multiple-oscillation gray soliton solution is identical to a Bogoliubov phonon, which has a discrete spectrum in the toroidal environment. If we choose the case that $l = 0$ —a nonrotating background—then the phonon group velocity in the long-wavelength limit is equal to the critical velocity, since

$$v_c = \lim_{n \rightarrow 0} \frac{d\delta\omega}{dn} = \sqrt{2\alpha}. \quad (4.28)$$

Shorter-wavelength phonons travel at velocities $v > v_c$. These correspond to the low-amplitude limit of multiple-soliton solutions with more kinks. As the amplitude increases, these solutions become nonlinear and turn into single- and multiple-kink solitons, which we treat in greater detail in the following section.

V. KINK SOLITONS

From now on we consider the repulsive case $\alpha > 0$. This means that the scattering length is positive and the interparticle interaction is repulsive. The Newtonian motion in the potential $V(f)$ is bounded only if the energy is less than a barrier height so that $E < E_0$, where

$$E_0 \equiv V(f_0) = \frac{\beta^2}{4\alpha} \quad (5.1)$$

corresponds to the top of the barrier, and we have introduced a constant f_0 defined as

$$f_0^2 \equiv \beta/\alpha. \quad (5.2)$$

The turning points are the roots of

$$E - V(f) = 0, \quad (5.3)$$

which yields the possible solutions f_1, f_2 , with

$$\begin{aligned} f_1^2 &= f_0^2 - B_0, \\ f_2^2 &= f_0^2 + B_0, \end{aligned} \quad (5.4)$$

where

$$B_0 = \frac{\beta}{\alpha} \sqrt{1 - \frac{E}{E_0}}. \quad (5.5)$$

The turning points of interest for dark solitons are actually at $f = \pm f_1$.

The boundary condition requires that, when $\bar{\theta}$ increases by 2π (from $-\pi$ to π), $f(\bar{\theta})$ changes sign if l is half-integer, and remains the same if l is integer. In the simplest case, f goes from $-f_1$ to f_1 for half-integer l . For the dark soliton (with half-integer l), noting that the integrals are all even in f , we have from Eq. (4.12)

$$\begin{aligned} \int_{-\pi}^{\pi} d\bar{\theta} &= \int_{-f_1}^{f_1} \frac{df}{\sqrt{2[E - V(f)]}} \\ &= 2\sqrt{\frac{2}{\alpha}} \int_0^{f_1} \frac{df}{\sqrt{(f_1^2 - f^2)(f_2^2 - f^2)}}. \end{aligned} \quad (5.6)$$

This condition gives a relation between E and ω . The normalization condition then determines ω .

Let us define

$$G(f) = \int_0^f \frac{dx}{\sqrt{(f_1^2 - x^2)(f_2^2 - x^2)}}. \quad (5.7)$$

Then the boundary condition can be stated in the form

$$G(f_1) = \pi \sqrt{\frac{\alpha}{2}}. \quad (5.8)$$

The solution $f(\bar{\theta})$ is then given by the implicit equation

$$\bar{\theta} = \sqrt{\frac{2}{\alpha}} G(f). \quad (5.9)$$

The integral we have for $G(f)$ can be expressed in terms of the Jacobi-elliptic function

$$\text{sn}^{-1}(x/b) = a \int_0^x \frac{dt}{\sqrt{(a^2 - t^2)(b^2 - t^2)}}. \quad (5.10)$$

The explicit solution is therefore

$$f(\bar{\theta}) = f_2 \text{sn} \left(f_1 \sqrt{\frac{\alpha}{2}} \bar{\theta} \right). \quad (5.11)$$

The width of the soliton is of the order of

$$\Delta\theta = \frac{1}{f_1} \sqrt{\frac{2}{\alpha}}. \quad (5.12)$$

Since $\alpha \propto N$ we have, for large N :

$$\Delta\theta \propto 1/\sqrt{N}, \quad (5.13)$$

i.e., the soliton becomes narrower as the number of particles increases.

VI. LIMITING tanh SOLITON

While the elliptic-function solution is the correct solution to the dark soliton problem, it tends to lack intuition. It is simpler to consider the limiting case of a soliton that is narrow compared to the torus circumference, where an approximate tanh solution is obtained.

Consider the limiting case $E \rightarrow E_0$, in which $B_0 \rightarrow 0$ and

$$\begin{aligned} f_1 &= \sqrt{f_0^2 - B_0} \approx f_0 \left(1 - \frac{B_0}{2f_0^2} \right), \\ f_2 &= \sqrt{f_0^2 + B_0} \approx f_0 \left(1 + \frac{B_0}{2f_0^2} \right). \end{aligned} \quad (6.1)$$

Setting $B_0 = 0$ in the above expressions, we can make the approximation that

$$G(f) \approx \int_0^f \frac{dx}{f_0^2 - x^2} = \frac{1}{2f_0} \sqrt{\frac{2}{\alpha}} \ln \left| \frac{f_0 + f}{f_0 - f} \right| = \frac{1}{f_0} \tanh^{-1} \left(\frac{f}{f_0} \right). \quad (6.2)$$

This leads to the explicit solution

$$f(\bar{\theta}) \simeq \sqrt{\frac{\beta}{\alpha}} \tanh\left(\sqrt{\frac{\beta}{2}} \bar{\theta}\right), \quad (6.3)$$

which is easily verified to be an exact solution of the original Newtonian effective particle equation, apart from the discontinuous derivative occurring at $\bar{\theta} = \pm \pi$. The boundary condition $G(f_1) = \pi\sqrt{\alpha/2}$ requires

$$\frac{2\beta^2}{\sqrt{\alpha(E_0 - E)}} = \exp(2\pi\sqrt{\beta/2}). \quad (6.4)$$

The normalization condition $\int_{-\pi}^{\pi} d\theta f^2 = 2\pi$ gives

$$\frac{\beta}{\alpha} \int_{-\pi}^{\pi} d\theta \tanh^2(\sqrt{\beta/2}\theta) = 2\pi. \quad (6.5)$$

The last two equations determine E and β , and therefore give the relation between E and ω .

Consider now the large N limit. Since $\tanh^2 x < 1$, we have the following inequality,

$$\int_{-\pi}^{\pi} d\theta \tanh^2(\sqrt{\beta/2}\theta) < 2\pi. \quad (6.6)$$

The normalization requires $\beta > \alpha$, or $\beta > 4NRa/A$. Therefore, $\beta \rightarrow \infty$ as $N \rightarrow \infty$. In this limit the dark soliton becomes infinitely narrow, and we can carry out the normalization integral to obtain

$$1 = \frac{\beta}{2\pi\alpha} \int_{-\pi}^{\pi} d\theta \tanh^2(\sqrt{\beta/2}\theta) \simeq \frac{\beta}{\alpha} \left(1 - \frac{1}{\pi\sqrt{\beta/2}}\right). \quad (6.7)$$

This leads to the limiting result that

$$\beta \simeq \alpha \left(1 + \frac{1}{\pi} \sqrt{\frac{2}{\alpha}}\right). \quad (6.8)$$

A. Limiting gray soliton

We can also obtain the corresponding gray-soliton result through direct substitution into the complex Newton's equations, of an ansatz of form

$$f(\bar{\theta}) \simeq a e^{ik\bar{\theta}} [\sqrt{1-b^2} + ib \tanh(bc\bar{\theta})]. \quad (6.9)$$

This leads to the result that for a limiting gray soliton with amplitude a , the quantities k and c are determined by the following equations:

$$\begin{aligned} c &= a \sqrt{\frac{\alpha}{2}}, \\ k &= c \sqrt{1-b^2}. \end{aligned} \quad (6.10)$$

If $b = 1$, this corresponds to the dark-soliton result given above. In the limit of large α , we also must take $a = 1$ for

normalization. It is interesting to compare the result for a low-amplitude isolated gray soliton (i.e., $b \rightarrow 0$) with the result for a long-wavelength phonon. If we make the background stationary by setting $l = -k = -c$, then the kink velocity is $v = 2c$. But, in this limit $c = \sqrt{\alpha/2}$ so that $v = v_c = \sqrt{2}\alpha$. In other words, an isolated low-amplitude gray soliton travels at the same velocity as a long-wavelength phonon.

As the amplitude of the kink increases, the velocity reduces relative to the background condensate. However, at the same time it is necessary to introduce a finite background velocity to satisfy the boundary conditions. The final result is that one obtains a dark soliton moving at the background velocity, but with a condensate that must itself be circulating in order to give a continuous phase.

B. Conserved quantities

We can now estimate values of the conserved quantities that characterize the dark soliton with periodic boundaries. The energy can be calculated by using the approximation that $f(\theta) \simeq \sqrt{\beta/\alpha} \tanh(\sqrt{\beta/2}\theta)$. This substitution must be carried out carefully, since the large size of α means that any small error in f can lead to a large error in the nonlinear term contributing to the energy. For this reason, we turn to the third expression for the energy calculated above, Eq. (4.10), which gives that, to leading order

$$\epsilon = \frac{\beta}{2} + l^2 + \frac{\alpha}{8\pi} \int_{-\pi}^{\pi} d\theta \operatorname{sech}^4(\sqrt{\alpha/2}\theta). \quad (6.11)$$

Next, we must use the approximate expression for β , valid at large N , obtained above. This combination gives us the final result that

$$\epsilon = \frac{\alpha}{2} + \frac{\sqrt{8\alpha}}{3\pi} + l^2 + O(1). \quad (6.12)$$

The energy and angular momentum for a single tanh soliton and a vortex state are given below for comparison.

For narrow solitons

$$\begin{aligned} \epsilon^{\text{soliton}} &\simeq \frac{\alpha}{2} + \frac{\sqrt{8\alpha}}{3\pi} + l^2 + O(1), \\ j^{\text{soliton}} &= l \left(\frac{1}{2}, \frac{3}{2}, \frac{5}{2}, \dots \right). \end{aligned} \quad (6.13)$$

For vortices or uniformly rotating condensates with integer angular momentum

$$\begin{aligned} \epsilon^{\text{vortex}} &= \frac{\alpha}{2} + l^2, \\ j^{\text{vortex}} &= l \quad (l = 1, 2, 3, \dots). \end{aligned} \quad (6.14)$$

The soliton spectrum begins at $\alpha/2 + \sqrt{8\alpha}/3\pi + \frac{1}{4}$, while that for vortex states begins at $\alpha/2 + 1$, i.e., the soliton spectrum starts lower than the vortex spectrum if $\sqrt{8\alpha}/3\pi < \frac{3}{4}$, or

$\alpha < 6.2$. Of course, this value is only approximate as it is derived using an approximate form of the soliton. In other words, the dark-soliton spectrum is expected to have a lower energy than that for vortex states for weakly repulsive interactions, because the lowest-soliton state has $j = 1/2$, whereas the lowest-vortex state has $j = 1$. However, there is an additional energy due to the compression of the condensate caused by the increase in density in the “bright” region of the soliton, to allow the low density hole to form at the phase singularity. This effect is larger than the increased kinetic energy of the vortex if α is large; although not if α is small. Both effects become vanishingly small relative to the bulk energy of the condensate in the limit of large N , as the singularity of the soliton core occupies a smaller and smaller region.

VII. GAIN-LOSS MECHANISM AND ATOM LASER MODE LOCKING

We have described a periodic motion in the ring-shaped condensate corresponding in the repulsive case to a kink soliton. To make use of this configuration in an atom laser we have to consider a more realistic setting by adding gain and loss mechanisms and show that this configuration is robust against perturbations. While creating a cw gain mechanism is still in the process of development, output coupling can be readily realized, for example, through a local Raman-tuned transition to a nontrapped state of the atoms. In this situation it would be important to stabilize the relative phase of the two Raman laser beams in order to maintain a stable condensate phase in the output atom-laser pulse train.

In experimental situations, the condensate is in equilibrium with a thermal cloud of uncondensed atoms. The equilibrium number of condensate atoms, relative to that in the thermal cloud, depends on the temperature and it determines the width of the soliton. A loss of particles from the condensate will tend to increase the width, but this will be countered by a gain from the thermal cloud. The kink soliton can withstand this type of external perturbations, because of a topological stability, for it cannot be continuously deformed into a uniform state. Thus, with appropriate gain and loss mechanisms, we can create a self-maintained soliton and a steady stream of coherent output pulses.

First, we create a dark soliton with $l = 1/2$ from a uniform static condensate, by momentarily stirring it at the soliton velocity $v = 1$. In practice, this can be produced by a blue-detuned laser beam. In the numerical simulation, we introduce an external repulsive potential $\mathcal{V}(\theta, \tau)$ to create a moving “hole” in the condensate at $\theta = \tau - \pi$. The time origin is displaced by π , to wait for the hole to fully form. Next, we have to clean up the configuration by adding gain and loss mechanisms, for the stirring creates other excitations such as phonons, in addition to the dark soliton. The entire procedure is contained in the generalized equation of motion

$$i \frac{\partial \psi}{\partial \tau} = - \frac{\partial^2 \psi}{\partial \theta^2} + \alpha |\psi|^2 \psi + \mathcal{V}(\theta, \tau) \psi + i [g - \gamma(\theta, \tau)] \psi, \quad (7.1)$$

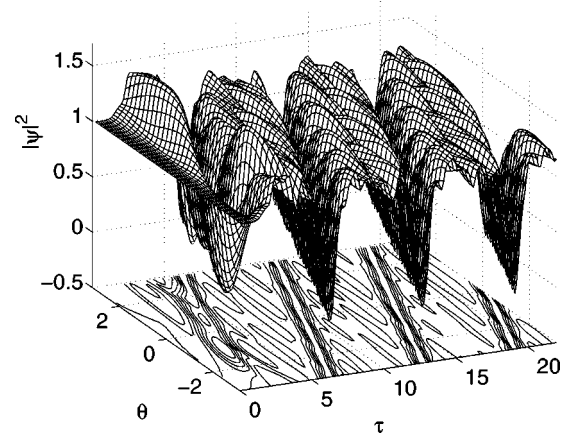


FIG. 1. Density of the condensate $|\psi|^2$ as a function of the angle around the ring and dimensionless time. Stirring an initially uniform condensate at the soliton velocity creates a moving hole, which develops into a dark soliton after unwanted excitations are cleaned by the loss mechanism. The soliton survives because of topological stability as a kink.

where the stirring potential is given by

$$\mathcal{V}(\theta, \tau) = \mathcal{V}_0 \exp \left[- \left(\frac{\theta - \tau + \pi}{\sigma_1} \right)^2 - \left(\frac{\tau - \pi}{\sigma_2} \right)^4 \right], \quad (7.2)$$

In the gain-loss mechanism g is a constant gain rate, representing stimulated emission from noncondensed atoms that are continuously loaded into the trap. The loss function makes localized periodic hits at the center of the soliton

$$\gamma(\theta, \tau) = \gamma_0 \exp \left[- \left(\frac{\theta}{\sigma_\theta} \right)^2 - \left(\frac{\tau_1}{\sigma_\tau} \right)^2 \right], \quad (7.3)$$

where $\tau_1 = \text{mod}_{2\pi}(\tau) - \pi$. This simulates a stroboscopic output coupler. The strobe acts for the first time with the center at $\tau = 3\pi$, allowing time for the hole to form.

A. Numerical results

The feasibility of the scheme described above can be demonstrated by numerical simulations, as we now describe.

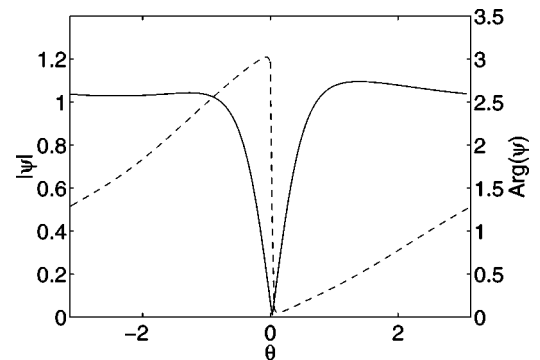


FIG. 2. Modulus and phase of the dark soliton as functions of the angle around the ring at a time when it has become fully stabilized. The phase jumps by π across the dip indicating that the soliton is a kink.

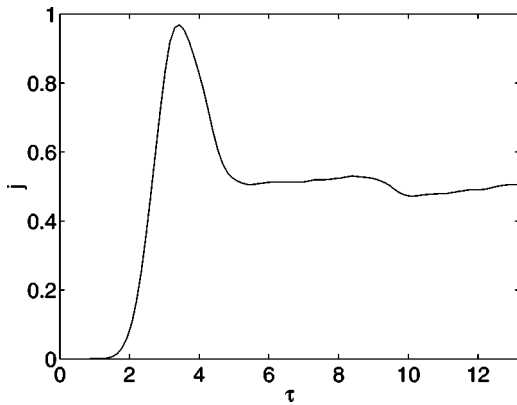


FIG. 3. The dimensionless angular momentum j goes through transients while the condensate is being stirred, but stabilizes to a value around $1/2$ characteristic of a kink under actions of the gain-loss mechanism.

We set $\alpha=7.363$, which corresponds to $\beta=8.69$ in Eq. (6.7). For the stirring potential we use $\mathcal{V}_0=12.3$, $\sigma_1=0.788$, and $\sigma_2=\pi/2$. We use a gain rate of $g=0.01$, and set the loss parameters to $\gamma_0=0.9$, $\sigma_\theta=1.1\sqrt{2/\beta}$, and $\sigma_\tau=1.1\sqrt{2/\beta}$.

Following are the results of numerical calculations, with the initial condition $\psi=1$. Figure 1 shows $|\psi|$ as a function of θ and τ . We see that a hole is formed and it develops into a dark soliton through the action of the gain-loss mechanisms. A more detailed view is shown in Fig. 2, which shows $|\psi|$ and the phase of a mode-locked soliton as a function of θ at a fixed time. The signature is that the phase jumps by π across the soliton. The modulus does not precisely vanish due to small admixtures of nonsoliton excitations. Figure 3 shows the dimensionless angular momentum per particle j , which rises from 0 to almost 1 as the condensate is being stirred, but settles down to $1/2$, characteristic of a kink, under actions of the gain-loss mechanism. Figure 4 shows the total number of atoms in the ring as a function of time. The steady-state oscillations indicate an output train of pulses with a stabilized intensity. In addition, a calculation of the condensate phase shows that the phase difference from pulse to pulse remains unchanged, i.e., that the atom laser pulses are coherent with each other. In this simulation, the stroboscope performs the dual task of cleaning up the soliton and acting as out coupler for the mode-locked laser. In general, these tasks could be done by separate mechanisms.

Our numerical results are quite sensitive to the exact strength of the inter-atomic repulsive potential. In actual experiments, however, one can adjust the potential either by taking advantage of the similar couplings that exist in two-component Bose gases [11] or by using tuning techniques involving Feshbach resonances [12], which have been re-

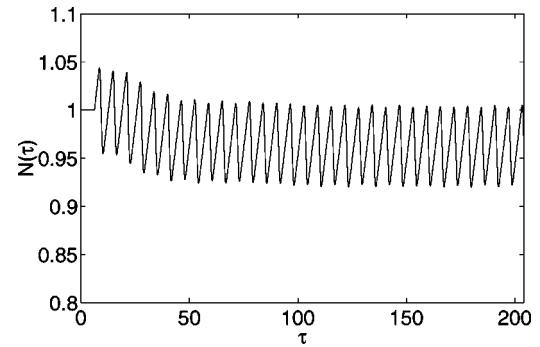


FIG. 4. Mode locking—production of a coherent train of pulses—is indicated by the steady-state oscillation of the total number of atoms in the condensate.

cently demonstrated experimentally [13].

VIII. SUMMARY

In summary, the soliton can form as a circulating, kinklike solution, which has the unexpected property that it has a fractional (half-integer) angular momentum per particle. This is stable in a rotationally symmetric environment and, in fact, numerical simulations indicate that it is also relatively stable with small (adiabatic) departures from rotational symmetry. However, as it has a higher energy than the nonrotating ground state, one might expect that in an environment that does not conserve angular momentum, it is possible for a decay to occur to the nonrotating state. This would presumably occur via the creation of a gray soliton, which can have a lower angular momentum than the dark, tanh-type soliton.

By using gain and an appropriately synchronized periodic output coupler it may be feasible to stabilize the dark soliton to create an atom laser with a reproducible, coherent waveform. This allows one possible route towards manufacturing a mode locked, pulsed-atom laser. The advantage of mode locking in lasers is that the all atom lasers to date have involved a pulsed output field. In a mode-locked laser the sequence of output pulses are in phase with each other. This allows a wide range of interference experiments and phase-sensitive measurements. In addition, mode-locked lasers can have an enhanced intensity stability compared to nonmode-locked lasers.

ACKNOWLEDGMENTS

We would like to acknowledge useful discussions with M. Holland. A.E. and K.H. were supported in part by DOE Cooperative Agreement No. DE-FC02-94ER40818. P.D. and K.K. acknowledge the support by the Australian Research Council.

[1] M. H. Anderson, J. R. Ensher, C. E. Wieman, and E. A. Cornell, *Science* **269**, 198 (1995); C. C. Bradley, C. A. Sackett, J. J. Tollett, and R. G. Hulet, *Phys. Rev. Lett.* **75**, 1687 (1995); K. B. Davis, M.-O. Mewes, M. R. Andrews, N. J. van Druten,

D. S. Durfee, D. M. Kurn, and W. Ketterle, *ibid.* **75**, 3969 (1995); K. Burnett, *Contemp. Phys.* **37**, 1 (1996); K. B. Davis, M. O. Mewes, and W. Ketterle, *Appl. Phys. B: Lasers Opt.* **60**, 155 (1995).

- [2] M. R. Andrews *et al.*, *Science* **275**, 637 (1997); M.-O. Mewes *et al.*, *Phys. Rev. Lett.* **78**, 582 (1997); B. P. Anderson and M. A. Kasevich, *Science* **282**, 1686 (1998); I. Bloch, T. W. Haensch, and T. Esslinger, *Phys. Rev. Lett.* **82**, 3008 (1999); E. W. Hagley *et al.*, *Science* **283**, 1706 (1999).
- [3] M. Holland, K. Burnett, C. Gardiner, J. I. Cirac, and P. Zoller, *Phys. Rev. A* **54**, R1757 (1996); R. J. C. Spreeuw *et al.*, *Europhys. Lett.* **32**, 469 (1995); H. Wiseman and M. J. Collet, *Phys. Lett. A* **202**, 246 (1995); A. M. Guzman, M. Moore, and P. Meystre, *Phys. Rev. A* **53**, 977 (1996); G. M. Moy, J. J. Hope, and C. M. Savage, *ibid.* **55**, 3631 (1997); H. M. Wiseman, *ibid.* **56**, 2068 (1997); R. J. Ballagh, K. Burnett, and T. F. Scott, *Phys. Rev. Lett.* **78**, 3276 (1997); B. Kneer *et al.*, *Phys. Rev. A* **58**, 4841 (1998); Y. B. Band, P. S. Julienne, and M. Trippenbach, *ibid.* **59**, 3823 (1999).
- [4] B. P. Anderson and M. A. Kasevich, *Science* **282**, 1686 (1998).
- [5] A. Hasegawa, *Optical Solitons in Fibers*, 2nd ed. (Springer-Verlag, Berlin, 1995).
- [6] M. Ueda and K. Huang, *Phys. Rev. A* **60**, 3317 (1999); A. Eleftheriou and K. Huang, *ibid.* **61**, 043601 (2000).
- [7] W. P. Reinhardt and C. W. Clark, *J. Phys. B* **30**, L785 (1997); T. F. Scott, R. J. Ballagh, and K. Burnett, *ibid.* **31**, L329 (1998); A. D. Jackson, G. M. Kavoulakis, and C. J. Pethick, *Phys. Rev. A* **58**, 2417 (1998); P. O. Fedichev, A. E. Muryshv, and G. V. Shlyapnikov, *ibid.* **60**, 3220 (1999); T. Busch and J. R. Anglin, *Phys. Rev. Lett.* **84**, 2298 (2000).
- [8] S. Burger *et al.*, *Phys. Rev. Lett.* **83**, 5198 (1999).
- [9] J. Denschlag *et al.*, *Science* **287**, 97 (2000).
- [10] N. Bogoliubov, *J. Phys. (Moscow)* **11**, 23 (1947).
- [11] T.-L. Ho and V. B. Shenoy, *Phys. Rev. Lett.* **77**, 3276 (1996); B. D. Esry *et al.*, *ibid.* **78**, 3594 (1997); C. K. Law, H. Pu, N. P. Bigelow, and J. H. Eberly, *ibid.*, **79**, 3105 (1997); Th. Busch *et al.*, *Phys. Rev. A* **56**, 2978 (1997); H. Pu and N. P. Bigelow, *Phys. Rev. Lett.* **80**, 1130 (1998); P. Öhberg, *Phys. Rev. A* **59**, 634 (1999); C. J. Myatt *et al.*, *Phys. Rev. Lett.* **78**, 586 (1997); D. S. Hall *et al.*, *ibid.* **81**, 1539 (1998); D. S. Hall, *et al.*, *ibid.* **81**, 1543 (1998).
- [12] E. Tiesinga, B. J. Verhaar, and H. T. C. Stoof, *Phys. Rev. A* **47**, 4114 (1993); E. Tiesinga, A. J. Moerdijk, B. J. Verhaar, and H. T. C. Stoof, *ibid.* **46**, R1167 (1992); A. J. Moerdijk, B. J. Verhaar, and A. Axelsson, *ibid.* **51**, 4852 (1995); J. M. Vogels *et al.*, *ibid.* **56**, R1067 (1997); P. Tommasini, E. Timmermans, M. Hussein, and A. Kerman, e-print cond-mat/9804015.
- [13] S. Inouye *et al.*, *Nature (London)* **392**, 151 (1998); Ph. Courteille, R. S. Freeland, and D. Heinzen, *Phys. Rev. Lett.* **81**, 69 (1998); J. L. Roberts *et al.*, *ibid.* **81**, 5109 (1998); J. Stenger *et al.*, *ibid.* **82**, 2422 (1999).